From Root to Receptor : GC-MS Based Metabolite Identification and Docking - Guided Anticancer Evaluation of *Celosia* Root Extract.

H. Bhagyasri[1], B. Sujatha[2], J. Glory Hannah[3], Ch. Sowmithri[4], M. Kiran Kumar[5]

Addresses of Authors:

1. Research Scholar, Department of Botany, Andhra University, Visakhapatnam- 530003, Andhra Pradesh, India.
Mail. id: bhagyasrih456@gmail.com
2. Professor, Department of Botany, Andhra University, Visakhapatnam- 530003, Andhra Pradesh, India.
Mail. id: sujathaau@yahoo.co.in
3. Research Scholar, Department of Biotechnology, Andhra University, Visakhapatnam- 530003, Andhra Pradesh, India.
Mail.id: gloryjhannah@gmail.com
4. Research Scholar, Department of Botany, Andhra University, Visakhapatnam- 530003, Andhra Pradesh, India
Mail. id: chalugusowmithri@gmail.com
5. Director, SSR Biosciences, Adavivaram, Visakhapatnam-530028, Andhra Pradesh, India. Mail. id: kiran65@ssrbioscience.com

Corresponding Author
H. Bhagyasri

ABSTRACT

Cancer continues to be a major global health concern with millions of new cases and fatalities each year. Although patient outcomes have improved due to advancements in chemotherapy, radiotherapy, targeted therapy, and immunotherapy, their effectiveness is often limited by side effects, drug resistance, poor tumour selectivity, and high treatment costs. The search for safer and more potent anticancer drugs derived from plants thus received attention. This study evaluated the phytochemical composition and anticancer potential of the methanolic root extract of *Celosia argentea* by using phytochemical screening, gas chromatography-mass spectrometry (GC-MS), molecular docking, and in vitro cytotoxicity studies. Preliminary phytochemical screening indicated the presence of alkaloids, flavonoids, saponins, tannins, steroids, terpenoids, glycosides, phenolic compounds, carbohydrates, proteins and amino acids. GC-MS analysis revealed 253 chromatographic peaks in the retention time range of 3.64 – 32.88 min, of which thirteen representative compounds were selected for molecular docking. Six target proteins involved in cancer (BRCA1, HER2, β-catenin, CyclinB1, HPV E6, and EGFR) were tested with four compounds (ergostane-3,5,6,12,25-pentol 25-acetate, 1-methyldecahydronaphthalene, methyl stearate, and eicosene). Among these, Ergostane-3,5,6,12,25-pentol 25-acetate exhibited the strongest binding affinities of -6.6 to -9.5 kcal/mol, suggesting a favourable interaction with all the selected targets. The antiproliferative activity of the methanolic root extract was also observed against MCF-7, Hep3B, and HeLa cell lines in a concentration-dependent manner, with the maximum activity in the case of HeLa cells. These findings suggest that roots of *C. argentea* are a potential source of bioactive phytochemicals with multitarget anticancer activity. To confirm their therapeutic potential, more mechanistic research and isolation of the active ingredients are required.

How to cite this article: H. Bhagyasri. Title: From Root to Receptor : GC-MS Based Metabolite Identification and Docking - Guided Anticancer Evaluation of Celosia Root Extract.. Int J Drug Deliv Technol. 2026;16(89s):1039-1055. DOI: 10.25258/ijddt.16.89s.108.

INTRODUCTION

Cancer is a multi-factorial disease defined by excessive proliferation of malignant cells, resistance to programmed cell death (apoptosis), sustained angiogenesis, invasion and metastasis due to the accumulation of genetic and epigenetic alterations that affect key cellular signalling pathways [1]. In particular, natural products have gained great interest over the past few decades as a key source of structurally diverse bioactive molecules; two-thirds of all currently approved anticancer drugs are either natural products or their derivatives, or synthetic compounds that mimic the lead agents afforded by nature [2]. In addition, medicinal plants are an infinite reservoir of phytochemicals with different chemical structures and biological activities, raising their promise as candidates for new anticancer agent discovery and development [3].

Medicinal plants were integral parts of conventional healthcare systems for thousands of years and still constitute one of the most attractive sources to discover new drug treatments [4,5]. Their amazing chemical diversity has led to numerous secondary metabolites that are pharmacologically active and have played key roles in the development of contemporary medical therapies, especially for cancer [6]. These bioactive components were further divided into various sub-types with significant interest in the regulation of many biological processes involved in cancer development and progression, like apoptosis, cell-cycle arrest, inhibition of angiogenesis, modulation of oxidative stress and blockage of metastatic signalling pathways [7,8], which include alkaloids, flavonoids, terpenoids, steroids, phenolic compounds, saponins and glycosides. *Curcuma longa* showed well known

anticancer effects by the modulation of apoptosis, cell-cycle arrest, inflammation and various oncogenic signalling pathways [9]. Natural products thus played an important role in cancer therapy, with several clinically approved anticancer drugs such as paclitaxel, vincristine, vinblastine, camptothecin derivatives and podophyllotoxin analogues derived from plants [10,11].The essential role of medicinal plants in modern oncology is further demonstrated by the fact that anticancer drugs that have been approved for clinical use are derived from compounds found in plants such as *Catharanthus roseus, Camptotheca acuminata*, and *Podophyllum spp.* [3].

C. argentea L., belonging to the family Amaranthaceae, is found to grow abundantly in tropical and sub-tropical areas of America, Africa and Asia. Since time immemorial, it has been utilised in Indian Ayurvedic, Chinese, and African traditional systems of medicine for its efficacy in various diseases like inflammation, diseases related to digestion, diabetes, disorders of the liver, haemorrhoids, infected wounds and eye disorders [12]. Their varied applications and frequent usage in different cultures helped to study the medicinal efficacy of *C. argentea* with growing intensity, and the number of studies conducted on it reveals some significant therapeuticproperties such as antidiabetic, antioxidant, anti-inflammatory, hepatoprotective, antimicrobial effects [13]. Furthermore, recent research showed that it has good anticancer potential, therefore paving the path for further inquiry as a reservoir for new bioactive components for cancer treatment [14]. The diverse phytochemical profile of *C. argentea* highlights its significant function as a source of numerous bioactive compounds for use in drug discovery activities [3]. Thus, in this respect, this work attempted to describe the phytochemical profile of the methanolic extract of *C. argentea* roots using GC-MS analysis, interaction of a few selected phytocompounds with important target cancer-associated proteins by molecular docking and to assess its anticancer efficacy.

MATERIAL AND METHODS:

1. SAMPLE COLLECTION: Roots were isolated from disease-free, mature plants of *Celosia* grown in the fields of Konam Village, Cheedikada Mandal, Anakapalle district of Andhra Pradesh, India, which is situated at Long. 82.870174°E and Lat. 17.962738°N. Healthy and mature plants were carefully uprooted from the field by means of sterilised tools, and attached soil was carefully removed from the root sample and immediately put in a zip-lock plastic bag and brought to the laboratory. In the laboratory, the root samples were properly washed in tap water and then in distilled water and were then shade dried and stored for further use.

2. METHANOLIC EXTRACT PREPARATION: The roots were dried, powdered and extract was prepared with methanol following the method described by Sasidharan et al., [15]. The crude methanolic extract of root was concentrated by evaporation to dryness, and stored in airtight containers at 4 °C until phytochemical characterization and anticancer activity evaluations. For anticancer assays, concentrations ranging from 25µg/mL to 500µg/mL were prepared using DMSO as the solvent.

% of Extract yield = $\frac{m2}{m1} \times 100$

Where m1= weight of the shade-dried roots

m2= weight of the concentrated crude extract.

3. GC-MS ANALYSIS:

The phytochemical composition of the methanolic root extract of *Celosia argentea* was assessed using the Shimadzu GCMS-QP2010 Plus GC-2010 gas chromatography system. The concentrate of the extract was pre- filtered using a 0.22 µm filter membrane to remove the undissolved part. GC- MS analysis was performed using an HP-5MS capillary column (30m × 0.25 mm i.d. × 0.25µm film thickness) equipped with helium as the carrier gas at a flow rate of 1.0 ml/min. The injection volume was 1 L with splitting mode, and the injector temperature was held at 250°C. The initial temperature of the oven was set to 45°C for 1min with increasing at rate of10°C /min to 280 °C and held for 3min. The interface temperature was kept at 280 °C. The detection was performed using EI positive ion detection. The source temperature was kept at 200 °C and mass spectra were recorded from m/z 40-700. The regions of the chromatogram, 3.643-32.880 min, were analysed and assigned to individual components.

Solvent cut-off time was programmed to 3.0 min to prevent interference with analysis from solvent peaks. The mass spectra were searched against NIST 14 and Wiley 8 mass spectrallibraries to tentatively identify the compounds based on matching factor with appropriate mass spectral libraries. Peak area normalisation based on TIC was used for calculation of percentage relative content for each identified phytochemical component.

MOLECULAR DOCKING

To analyse the binding between phytoconstituents obtained by GC-MS and some breast cancer, gastric cancer, and cervical cancer-specific proteins, a detailed molecular docking analysis was carried on 13 identified compounds by acquiring the three-dimensional crystal structure of some selected cancer target proteins (BRCA1; PDB ID: 1Y98, and HER2; PDB ID: 5KWG) for breast cancer,; β-catenin (PDB ID: 6O9C), and Cyclin B1 (PDB ID: 4Y72) for gastric cancer, and HPV E6 (PDB ID: 4GIZ) and EGFR (PDB ID: 1M17) for cervical cancer from the Protein Data Bank (PDB) [16]. The selected ligand molecules were procured in SDF format from the PubChem database [17].

The crystal structures of proteins were prepared to remove water, co-crystallised ligands, and other heterogeneous molecules using AutoDock Tools [18]. Before performing the docking operation, all selected ligands were subjected to energy minimisation, followed by conversion to the appropriate format for the subsequent docked system. Molecular docking between compounds obtained and target proteins was carried out using AutoDock Vina

to predict their docking binding affinity for target proteins [19]. A box (29, 26, 32Å for BRCA1; 25, 28, 24Å for HER2; 36, 29, 36Å for; β-catenin; 34, 26, 38Å for Cyclin B1; 38, 34, 40Å for HPV E6; 29, 34, 27Å for EGFR) centered around the active site of the protein with a spacing of 0.375 Å was generated. The lowest binding energy of the docking conformation for each compound-protein complex was selected since higher binding energies (less negative) result in less stable interactions [20]. Furthermore, binding interactions, including the formation of hydrogen bonds, hydrophobic contacts, and involvement of particular amino acids in the binding pocket, were studied. Additionally, molecular interactions between the docked complex, along with the orientation of ligands within the binding pockets, were analysed using the PyMOL Molecular Graphics System [21].

IN VITRO ANTICANCER STUDIES

The extract of *C. argentea* was subjected to evaluate the viability and cytotoxicity of cells by using a popular colourimetric approach against three human cancer cell lines, viz. MCF-7 (human breast adenocarcinoma), HeLa (cervical carcinoma), and Hep3B (hepatocellular carcinoma) using the MTT assay [22].The cell lines used were grown in Minimum Essential Medium (MEM) supplemented with 10% foetal bovine serum (FBS) and 1 Antibiotic-Antimycotic solution (HiMedia, India) in a humidified CO incubator at 37C with 5% CO [23]. The log-phase growth cells were detached and suspended in sterile 96-well microplates, then cultured overnight to enable cells to adhere to the well bottom.

After proper attachment, the culture medium was decanted and replaced with medium containing varied concentrations **(6.25, 12.5, 25, 50 and 100µg/mL)** of C. argentea extract. Untreated cells acted as a negative control, whereas cells treated with a standard anticancer drug agent worked as a positive control. The culture plates were then incubated for 24 h at 37C, 5% CO, humidified conditions to observe the effect of C. argentea on cancer cells. At the end of 24 h, the culture medium was supplemented with 0.5mg/mL MTT solution in 1 phosphate-buffered saline (PBS), and the culture was further incubated for 4 h at 37C, during which viableells reduced the yellow tetrazolium salt to purple formazan crystals by mitochondrial dehydrogenase activity [24]. The MTT solution was carefully discarded, and the wells were washed twice with 200 µL PBS to eliminate unincorporated stain. The purple crystals of formazan were dissolved in 100 µL DMSO after gentle stirring to make the solution homogeneous. The OD of formazan crystals was read at 570 nm in a microplate reader, and cell viability of treatment groups was calculated. Cytotoxic activity is the result of inhibition in the proliferation of cancer cells. So, the percentage of inhibition of the proliferation of cells was calculated using the formula:

% Inhibition = 100[(Mean OD of treated sample / Mean OD of control) 100]

RESULTS AND DISCUSSIONS GC-MS ANALYSIS

Analysis of the phytochemical components of the methanolic root extract of *Celosia argentea* was determined through Gas Chromatography-Mass Spectrometry (GC-MS), a well-established analytical technique in the separation of a variety of volatile and semi-volatile compounds present in plant matrices [25]. GC-MS was able to generate a well-separated chromatogram with well-shaped peaks to resolve the total ion chromatogram (TIC), where diverse ranges of compounds from 3.643 to 32.880 minutes have appeared on the GC-MS profile of methanolic root extract, which is reflected due to compounds of high, low, moderate, or low molecular weight and moderate or low volatility (Table 1), as it was reflected by wide ranges of RT and gave 253 chromatogram peaks indicating its richness of secondary phytochemicals (Figure 1). Identified constituents and associated peaks, retention time (RT), area %, height, molecular formula, molecular weight, and probable compound name for the methanolic extract were represented in Table 1. For identification of peaks, the mass fragmentation of these compounds was compared with those obtained from Wiley 8 and NIST 14 mass spectral libraries. It has been widely observed that methanol is considered a polar protic solvent, a moderate to low polar solvent, and a volatile extraction solvent that provides a wide range of compounds from moderately polar to low polar and to nonpolar with good extraction efficiency in obtaining phytochemicals from different parts of plants, especially including long-chain hydrocarbons, fatty acids, sterols, terpenoids, alcohols, aldehydes, ketones, phenolics, alkaloids, and heterocyclic compounds [26,27]. In total 253 compounds were detected in methanolic root extract of *Celosia argentea* by using GC-MS, and out of 253 compounds, seventeen significant representative compounds of the phytochemical profile, including 2-methyltetracosane (RT 23.824 min), dodecane (RT 10.484 min), 1-iodo-2-methylundecane (RT 7.740 min), 5-eicosene (RT 7.652 min), 2(3H)-furanone, dihydro- (RT 5.605 min), dimethyl sulfoxide (RT 5.205 min), 1-methyldecahydronaphthalene (RT 9.148 min), cyclohexane (RT 3.737 min), tetracosane (RT 24.451 min), ergostane-3,5,6,12,25-pentol, 25-acetate (RT 31.226 min), phytol (RT 24.250 min), octadecane (RT 19.488 min), tetratriacontane (RT 16.157 min), 5-chloropentanoic acid, 6-ethyl-3-octyl ester (RT 16.888 min), methyl stearate (RT 24.360 min), tricosane (RT 25.861 min), and squalene (RT 31.724 min), were tentatively identified, and there are some minor components throughout the entire process.

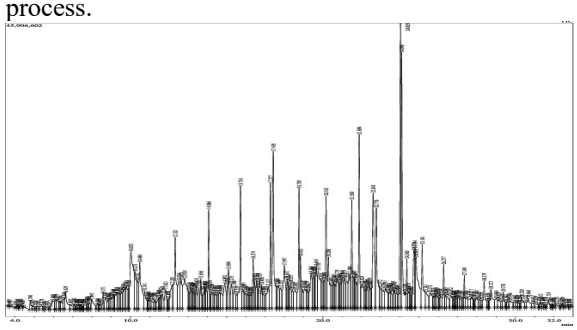


Figure 1. GC-MS Chromatogram of *C. argentea* methanolic root extract.

Phytochemical findings of the present study are in general consistent with the previous research of *C. argentea*, which indicated that the species is a rich source of many secondary metabolites that include sterols, triterpenoids, terpenoids, fatty acids, flavonoids, hydrocarbons, and other phenolic derivatives, all responsible for various medicinal activities [13]. Phytochemical components, including phytol, squalene, methyl stearate, tetracontane, tetracosane, methyl octadecanoate, ergostane-3,5,6,12,25-pentol, 25-acetate, and others found in our study, along with various other hydrocarbons and long-chain fatty acids and derivatives, possess different antioxidant, anti-inflammatory, antibacterial, antifungal, and anticancer effects [28]. Variations in constituents between the current study and prior reports may arise from differences in plant part, plant species, geographic source, cultivation techniques, extraction solvents, plant treatments, and analytical methodologies, as well as environmental conditions of the plants. Therefore, the identification of phytochemical constituents from the methanolic root extract of

C. argentea provides a solid foundation for additional exploration, including pharmacology assessment, virtual screening through molecular docking, and bioactivity-guided fractionation for potential therapeutic agent development [3].

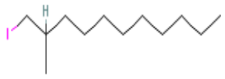
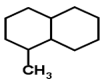
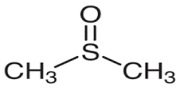
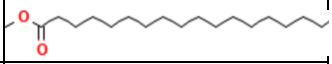
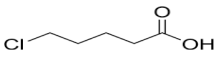
Table 1. GC-MS data of selected phytoconstituents from *C. argentea* methanolic root extract.

S. No	Compound	RT(min)	Peak Area (%)	Reported bioactivity
1	1-iodo 2-methylundecane	7.740	0.09	Antimicrobial property, estrogen-dependent chemo-signalling
2	1-methyldecahydronaphthalene	9.148	0.15	Used as a fragrance ingredient and fuel component
3	2(3H)-furanone	5.605	0.06	Anti-inflammatory, Analgesic, Antimicrobial, Antiviral, Anticancer
4	2-methyl tetracosane	23.824	0.28	Anticancer, Anti-inflammatory, Antioxidant
5	cyclohexane	3.737	0.01	Antibacterial, stimulates appetite
6	dimethyl sulfoxide	5.205	0.07	Anti-inflammatory, Analgesic, Antioxidant
7	dodecane	10.484	1.30	Used as an inert, lipophilic component
8	5-eicosene	7.652	0.09	Anticancer
9	ergostane-3,5,6,12,25-pentol,25-acetate	31.226	0.04	Anti-inflammatory, Analgesic, Antidiarrheal
10	methyl stearate	24.360	0.61	Neuroprotectant, Antioxidant, Anti-infection
11	octadecane	19.488	0.53	Antimicrobial, Antifungal
12	5-chloropentanoic acid	16.888	0.23	Anti-epileptic, Antiviral
13	tetratriacontane	16.157	0.19	Antibacterial, Antiviral
14	phytol	24.250	0.01	Antimicrobial, Anti-inflammatory, Antioxidant, Anticancer, Anxiolytic & Antinociceptive
15	tetracosane	24.451	0.31	Antimicrobial, Antioxidant
16	tricosane	25.861	0.19	Antibacterial, Antidiabetic
17	squalene	31.724	0.16	powerful antioxidant, anti-inflammatory, and immune-boosting

LIGAND SELECTION

The GC-MS analysis of the methanolic root extract of *Celosia argentea* reveals that there exist certain phytochemical constituents that have their own role in the therapeutic activity. Thirteen phytocompounds possessing reported biological activities were screened out from the detected metabolites of the extract, were subjected to molecular docking studies, viz., 1-iodo-2-methylundecane, 1-methyldecahydronaphthalene, 2(3H)-furanone, 2-methyltetracosane, 5-chloropentanoic acid, cyclohexane, dimethyl sulfoxide, dodecane, eicosene, ergostane-3,5,6,12,25-pentol,25-acetate, methyl stearate, octadecane and tetratriacontane. Table 2 summarises the information regarding the phytochemical ligands under investigation and their structure.

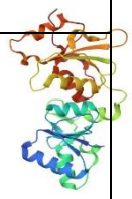
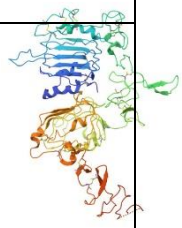
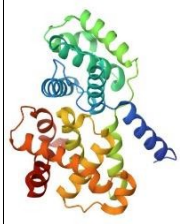
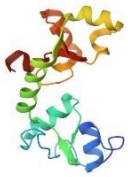
Table 2. Selected ligand molecules for molecular docking studies. **S. No**	**Compound Name**	**Structure**

1.	1-iodo 2-methylundecane	
2.	1-methyldecahydro naphthalene	
3.	2(3H)-furanone	
4.	2-methyl tetracosane	
5.	cyclohexane	
6.	dimethyl sulfoxide	
7.	dodecane	
8.	5-eicosene	
9.	ergostane-3,5,6,12,25-pentol,25-acetate	
10.	methyl stearate	
11.	octadecane	
12.	5-chloropentanoic acid	
13.	tetratriacontane	

ANTICANCER PROTEIN TARGETS

The selected anticancer target proteins (BRCA1, HER2, β-catenin, Cyclin B1, HPV E6 and EGFR) were retrieved from the Protein Data Bank (PDB). Before the molecular docking simulations, co-crystallised water molecules and heteroatoms were stripped out, and the protein structures were subjected to energy minimisation, resulting in stable receptor conformations toperform docking. The crystal structures and other information of the selected target proteins have been compiled in Table 3.

Table 3. Crystal structures of the selected anticancer target proteins from different cancers.

S. No	Type of cancer	Anticancer protein target	PDB ID	Structure
1.	Breast Cancer	BRCT (BRCA1 C-terminal phospho peptide)	**1Y98**	
		HER2 Receptor tyrosine-protein kinase erbB-2	**5KWG**	
2.	Gastric Cancer	Beta-catenin HLA class I histocompatibility antigen, A-3 alpha chain	**6O9C**	
		CyclinB1 G2/mitotic-specific cyclin-B1	**4Y72**	
3.	Cervical Cancer	HPVE6 Human papillomavirus Protein E6	**4GIZ**	
		EGFR Epidermal Growth Factor Receptor tyrosine kinase	**1M17**	

MOLECULAR DOCKING Molecular docking has been used extensively to predict the binding pose and affinity of small molecules to their protein targets, which is considered to give information about protein-ligand interaction and stability of complexes

[18,19]. In the present study, the thirteen phytocompounds obtained from GC–MS analysis of the methanolic root extract of *Celosia argentea* were docked against six anticancer target proteins; breast cancer-related proteins BRCA1 (PDB ID: 1Y98) and HER2 (PDB ID: 5KWG), gastric cancer-related proteins β - catenin (PDB ID: 6O9C) and Cyclin B1 (PDB ID: 4Y72), cervical cancer-related proteins HPV E6 (PDB ID: 4GIZ), and EGFR (PDB ID: 1M17). The docking affinity values were found in the range -2.1 kcal/mol to -9.5 kcal/mol for six proteins. Among the selected ligands, Ergostane-3,5,6,12,25-pentol,25-acetate showed the best interaction with all six selected protein targets showing high binding affinity value such as -7.1 kcal/mol for BRCA1, -9.4 kcal/mol for HER2, -8.6 kcal/mol for β-catenin, -9.5 kcal/mol for Cyclin B1, -6.6 kcal/mol for HPV E6 and -8.4 kcal/mol for EGFR. Also, compounds like 1-methyldecahydronaphthalene, methyl stearate and eicosene exhibited favourable docking energy against the selected proteins. It was found that the interaction energy of dimethyl sulfoxide and 2(3H)-furanone against the protein targets was lower, whereas 5-chloropentanoic acid and tetratriacontane had unstable conformations for the selected docking conditions. Therefore, the most effective four phytocompounds, namely ergostane-3,5,6,12,25-pentol,25-acetate, 1-methyldecahydronaphthalene, methyl stearate and 5-eicosene, were used to determine the docking-based interaction analysis. All docking energies of the thirteen phytocompounds against the selected anticancer targets are listed in Table 4.

Table 4. Binding affinities of the selected bioactive compounds and anticancer protein targets.

S.No	Ligands Of Root	Binding Affinity (kcal/mol)					
		Breast Cancer		Gastric Cancer		Cervical Cancer	
		BRCA 11 (1Y98)	HER 22 (5KWG)	BETACATEN IN (6O9C)	CYCLIN B 12 (4Y72)	HPV E6 (4GIZ)	EGF R (1M17)
1	1-iodo 2-methylundecane	-4.2	-5.6	-4.9	-5.9	-4.3	-4.5
2	1-methyldecahydronaphthalene	-4.8	-6.2	-5.8	-7.5	-5.7	-5.7
3	2(3H)-furanone	-3.6	-4.0	-3.9	-3.9	-3.4	-4.1
4	2-methyltetracosane	-4.8	-7.3	-5.4	-6.5	-4.3	-5.3
5	cyclohexane	-3.8	-4.7	-4.2		-5.2	-4.1 -3.7
6	dimethyl sulfoxide	-2.3	-2.9	-2.5	-2.3	-2.1	-2.3
7	dodecane	-4.6	-5.8	-4.9	-5.8	-4.7	-4.9
8	5-eicosene	-4.2	-6.7	-5.5	-6.1	-4.3	-5.0
9	ergostane-3,5,6,12,25-pentol,25-acetate	**-7.1**	**-9.4**	**-8.6**	**-9.5**	**-6.6**	**-8.4**
10	methyl stearate	-4.3	-6.8	-5.5	-6.7	-5.0	-5.0
11	octadecane	-4.1	-3.6	-4.5	-5.7	-4.3	-5.4
12	5-chloropentanoi c acid	Failed	Failed	Failed	Failed	Failed	Failed
13	tetratriacontan e	Failed	Failed	Failed	Failed	Failed	Failed

Interaction of ergostane-3,5,6,12,25-pentol,25-acetate with Anticancer Target Proteins

Based on the molecular docking analysis ergostane-3,5,6,12,25-pentol,25-acetate was selected for detailed protein–ligand interaction analysis because it exhibited favourable binding affinities against all six targets linked to cancer. Docking against BRCA1 (PDB ID: 1Y98), HER2 (5KWG), β-catenin (6O9C), Cyclin B1 (4Y72), HPV E6 (4GIZ), and EGFR (1M17)

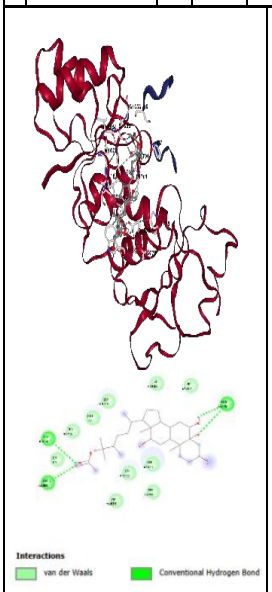
produced binding affinities of −7.1, −9.4, −8.6, −9.5, −6.6, and −8.4 kcal/mol respectively. Cyclin B1 showed the strongest binding, followed by HER2 and β-catenin; HPV E6 showed the weakest affinity. The ligand showed favourable accommodation within the predicted binding pockets and interacted with several key amino acid residues of the target proteins forming stable complexes with all six cancer-associated target proteins. The complete docking parameters, including binding affinities, cavity volumes, grid centre coordinates, and interacting amino acid residues, are summarised in Table 5, while the three-dimensional and two-dimensional binding poses of the docked complexes are illustrated in Figure 2, respectively. Overall, the consistent binding affinities across the six targets suggest the potential of ergostane-3,5,6,12,25-pentol,25-acetate as a multitarget anticancer candidate.

Table 5. Docking results of Ergostane-3,5,6,12,25-Pentol,25-acetate complex with selected anticancer protein targets.

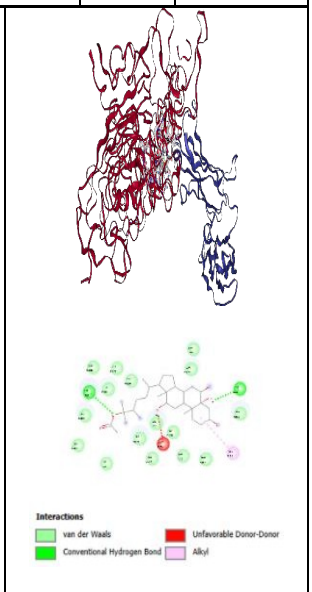
S. No	Ligand-Protein (PDB Id)	Vina Score	Cavity Volume	Centres XYZ	Docking Box XYZ	Residues

1.	Ergostane-3,5,6,12,25-Pentol,25-acetate - **1Y98**	-7.1	923	-27,51,05	25,25,25	**Chain A:** VAL 1654 SER 1655 GLY 1656 ASN 1678 LEU 1679 ILE 1680 THR 1700 LEU 1701 LYS 1702 LEU 1705 PRO 1776 ASP 1778 GLN 1779 TRP 1782
						Chain B: SER5 PRO7
2.	Ergostane-3,5,6,12,25-Pentol,25-acetate - **5KWG**	-9.4	3042	46,3,-16	25,25,25	**Chain C:** THR1 GLN2 VAL3 CYS4 THR5 GLN32 VAL33 GLN35 GLU57 ASN237 PHE269 GLY270 ALA271 SER272 VAL274 PRO278 TYR279 ASN280 TYR281 SER441 ARG465 ASN466 HIS468
3.	Ergostane-3,5,6,12,25-Pentol,25-acetate - **6O9C**	-8.6	3371	56,16,27	25,25,25	**Chain A:** TYR27 ASP29 ASP30 THR31 GLN32 ARG48 ALA49 ALA211 THR233 ARG234 PRO235 GLY237 ASP238 GLY239 PHE241 **Chain B:** TYR46 SER72 ASP73 TYR83 LEU85
4.	Ergostane-3,5,6,12,25-Pentol,25-acetate - **4Y72**	-9.5	1535	29,-66,190	25,25,25	**Chain A:** ILE10 GLY11 GLU12 TYR15 VAL18 ALA31 LYS33 GLU51 VAL64 PHE80 GLU81 ASP86 LYS88 GLN132 ASN133 LEU135 ALA145 ASP146
5.	Ergostane-3,5,6,12,25-Pentol,25-acetate – **4GIZ**	-6.6	366	-22, 67, -25	25, 25, 25	**Chain B**: TYR31 ASP48 LEU49 CYS50 VAL61 CYS65 LEU66 TYR69 SER70 SER73 LEU99 ARG101 GLN106 ARG128 GLY129 ARG130

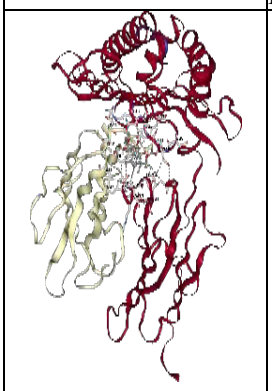
6.	Ergostane-3,5,6,12,25-Pentol,25-acetate – **1M17**	-8.4	665	24, 0, 54	25, 25, 25	**Chain A:** LEU694 GLY695 VAL702 ALA719 LYS721 GLU738 MET742 LEU764 THR766 LEU768 MET769 PRO770 PHE771 GLY772 CYS773 ASP776 TYR777 GLU780 HIS781 LEU820 THR830 ASP831



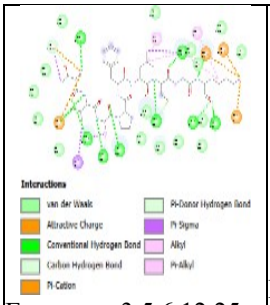
Ergostane-3,5,6,12,25-Pentol,25-acetate -**1Y98**



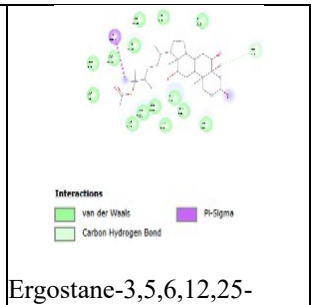
Ergostane-3,5,6,12,25-Pentol,25-acetate -**5KWG**



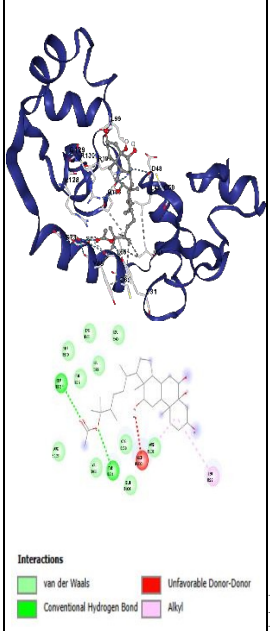




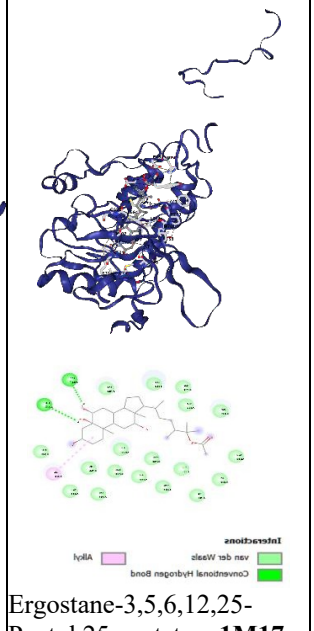
Ergostane-3,5,6,12,25-Pentol,25-acetate -**6O9C**



Ergostane-3,5,6,12,25-Pentol,25-acetate -**4Y7**



Ergostane-3,5,6,12,25-Pentol,25-acetate – **4GIZ**



Ergostane-3,5,6,12,25-Pentol,25-acetate – **1M17**

Figure 2. 3D and 2D interaction plots illustrating the binding interactions of Ergostane-3,5,6,12,25-Pentol,25-acetate within the active sites of the anticancer protein targets.

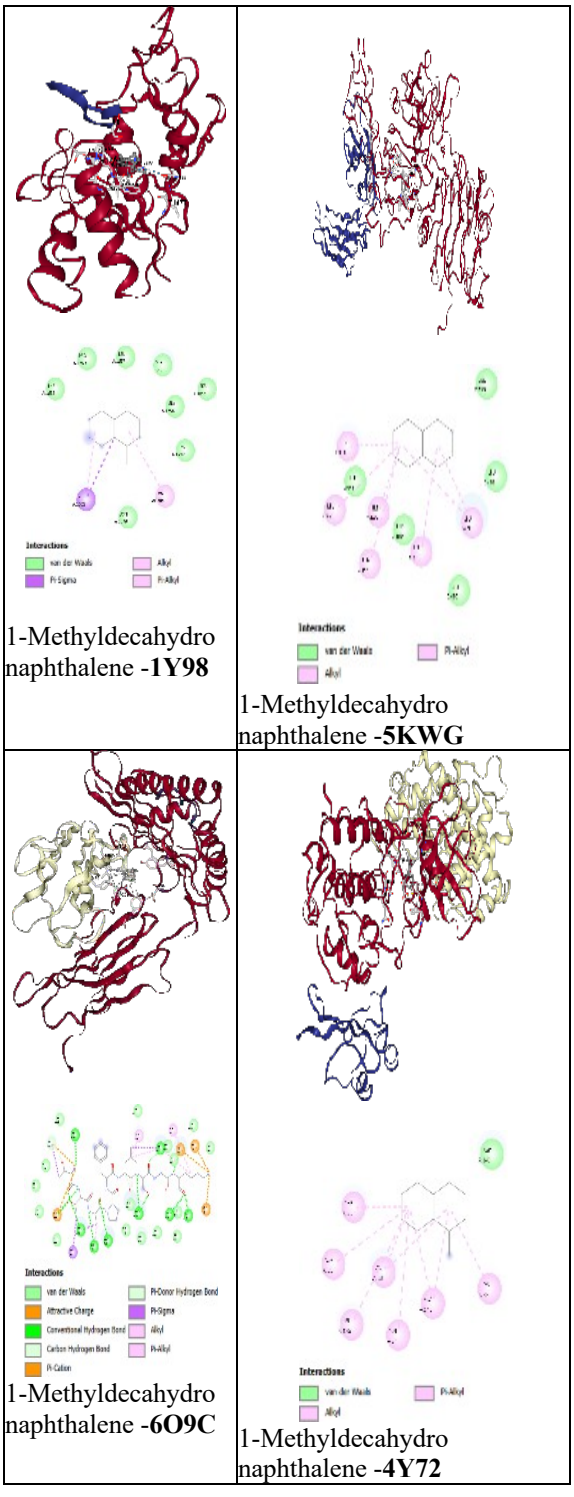
Interaction of 1-methyldecahydronaphthalene with Anticancer Target Proteins

Molecular docking analysis of1-methyldecahydronaphthalene exhibited favourable predicted binding with all six cancer-associated target proteins. Docking against 1-methyldecahydronaphthalene with BRCA1 (PDB ID: 1Y98), HER2 (PDB ID: 5KWG), β-catenin (PDB ID: 6O9C), Cyclin B1 (PDB ID: 4Y72), HPV E6 (PDB ID: 4GIZ), EGFR (PDB ID: 1M17) yielded binding affinities of-4.8, -6.2, -5.8, -7.5, -5.7, -5.7 kcal/mol respectively. Cyclin B1 showed strongest binding followed by HER2 and β-catenin, whereas BRCA1 showed the weakest affinity. Detailed docking parameters and interacting residues are presented in Table 6, while the corresponding three-dimensional and two-dimensionalinteraction poses are shown in Figure 3. Overall, the docking results indicate favourable interactions of 1-methyldecahydronaphthalene with multiple cancer-associated targets, supporting its

further evaluation for potential anticancer activity.

Table 6. Docking results of1-Methyldecahydro naphthalene complex with selected anticancer protein targets.

S. No	Ligand-Protein (PDB Id)	Vina Score	Cavity Volume	Centres XYZ	Docking Box XYZ	Residues
1.	1-Methyldecahydro naphthalene - **1Y98**	-4.8	923	-27,51,0	23,23,23	**Chain A:** VAL1654 SER1655 GLY1656 LEU1657 THR1658 PRO1659 THR1677 ASN1678 LYS1702 **Chain B:** SER5
2.	1-Methyldecahydro naphthalene - **5KWG**	-6.2	1037	43,24,-36	17,17,17	**Chain C:** LEU421 LEU423 LEU431 LEU433 LEU436 ALA444 LEU445 ILE446 TRP460 LEU471 TRP499
3.	1-Methyldecahydro naphthalene - **6O9C**	-5.8	3371	56,16,27	17,30,35	**Chain A:** TYR27 ASP30 GLN32 PRO235 GLY237 PHE241 **Chain B:** TYR46 SER72 TYR83 LEU84 LEU85
4.	1-Methyldecahydro naphthalene - **4Y72**	-7.5	1535	29,-66,190	17,27,29	**Chain A:** TYR15 VAL18 ALA31 LYS33 VAL64 PHE80 GLN132 ASN133 LEU135 ALA145 ASP146
5.	1-Methyldecahydro naphthalene - **4GIZ**	-5.7	374	-23,61,-16	17, 17, 17	**Chain B**: VAL30 TYR31 PHE44 LEU49 CYS50 VAL52 ALA60 VAL61 LEU66 TYR69
6.	1-Methyldecahydro naphthalene - **1M17**	-5.7	665	24, 0, 54	17, 17, 17	**Chain A:** VAL702 ALA719 ILE720 LYS721 GLU738 MET742 LEU764 THR766 LEU820 THR830 ASP831



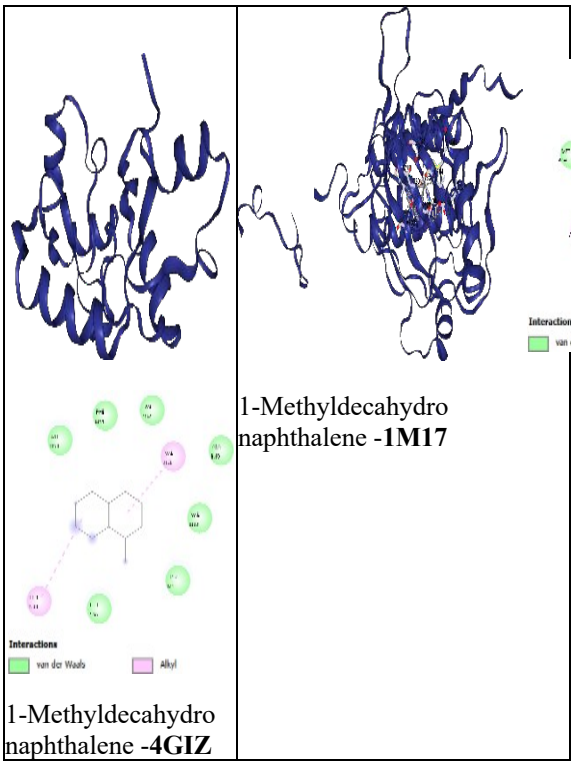


Figure 3. 3D and 2D interaction plots illustrating the binding interactions of 1-Methyldecahydro naphthalene within the active sites of the anticancer protein targets.

Interaction of Methyl stearate with Anticancer Target Proteins

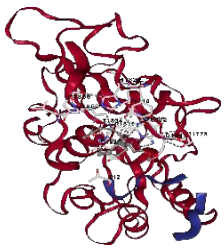
Methyl stearate was studied further against six cancer-related target proteins using docking to understand how it interacts within the areas where these proteins are active. The compound showed docking scores of −4.3 kcal/mol for BRCA1 (PDB ID: 1Y98) −6.8 kcal/mol for HER2 (5KWG) −5.5 kcal/mol for β- 6O9C) −6.7 kcal/mol for Cyclin B1 (4Y72) −5.0 kcal/mol for HPV E6 (4GIZ). −5.0 Kcal/mol for EGFR (1M17). The strongest interaction was found withHER2 with Cyclin B1 and β-catenin while BRCA1 had the weakest docking score. The full docking details and the residues involved in the interaction are listed in Table 7. The three-dimensional and two-dimensional views of how the molecule interacts are shown in Figure 4. Overall, the docking results indicate favourable interactions of methyl stearate with multiple cancer-associated targets and provide computational support for its further evaluation in anticancer studies.

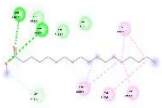
Table 7. Docking results of Methyl stearate complex with selected anticancer protein targets.

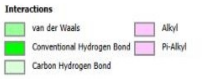
S. No	Ligand - Protein (PDB Id)	Vina Score	Cavity Volume	Centres XYZ	Docking Box XYZ	Residues

1.	Methyl stearate - **1Y98**	-4.3	166	-16,61,-2	26,26,26	**Chain A:** THR1773 VAL1810 GLN1811 PRO1812 ASP1813 PHE1821 HIS1822 THR1834 ARG1835 GLU1836 LEU1839 LEU1854 ILE1855 PRO1856 **Chain B:** THR12
2.	Methyl stearate - **5KWG**	-6.8	1037	43,24,-36	26,26,26	**Chain C:** LEU388 ILE390 LEU400 PHE403 LEU406 ILE409 LEU421 THR422 LEU423 LEU431 LEU433 LEU436 LEU445 ILE446 LEU452 PHE454 VAL455 VAL458 TRP460 LEU471 TRP499
3.	Methyl stearate - **6O9C**	-5.5	759	66,16,15	26,26,26	**Chain A:** ARG6 PHE8 TYR27 ASP29 ASP30 GLN32 ALA211 THR233 ARG234 PRO235 PHE241 **Chain B:** TYR46 SER72 ASP73 SER75 PHE76 TYR83 LEU85
4.	Methyl stearate - **4Y72**	-6.7	1535	29,-66,190	26,26,26	**Chain A:** ILE10 GLY11 GLU12 TYR15 VAL18 ALA31 LYS33 VAL64 PHE80 PHE82 LEU83 SER84 MET85 ASP86 LYS89 GLN132 ASN133 LEU135 ALA145 ASP146
5.	Methyl stearate – **4GIZ**	-5.0	374	-23, 61, -16	26, 26, 26	**Chain B:** VAL30 TYR31 PHE44 LEU49 CYS50 VAL52 ARG54 ALA60 VAL61 LEU66 TYR69 SER70 SER73 GLN106 ARG128 ARG130
6.	Methyl stearate - **1M17**	-5.0	991	36, 8, 51	26, 26, 26	**Chain A:** PHE699 VAL702 ALA719 ILE720 LYS721 LEU723 ALA731 GLU734 ILE735 GLU738 MET742 LEU764 ILE765 THR766

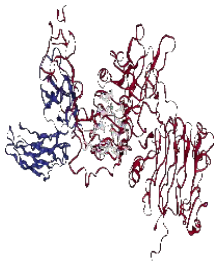
						LEU820 THR830 ASP831 GLY833

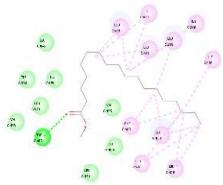


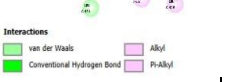




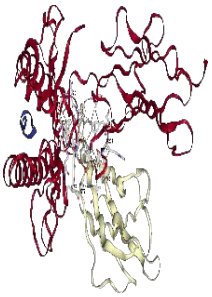
Methyl stearate -**1Y98**

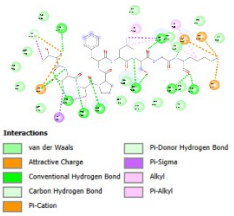




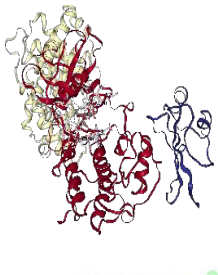


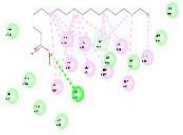
Methyl stearate-**5KWG**

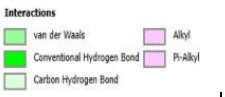




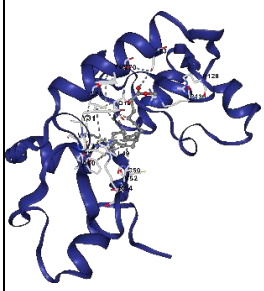
Methyl stearate - **6O9C**



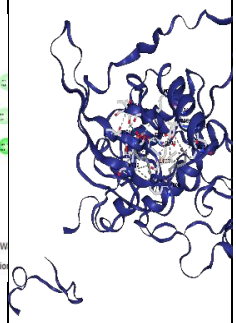




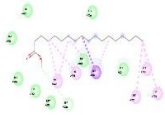
Methyl stearate - **4Y72**

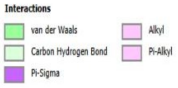






Methyl stearate – **4GIZ**





Methyl stearate – **1M17**

Figure 4. 3D and 2D interaction plots illustrating the binding interactions of Methyl stearate within the active sites of the anticancer target proteins.Interaction of Eicosene with Anticancer Target Proteins

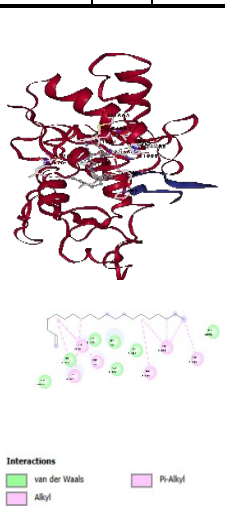
Molecular docking analysis of eicosene exhibited favourable predicted interactions with all six cancer-associated target proteins. Docking against eicosene with BRCA1 (PDB ID: 1Y98), HER2 (5KWG), β-catenin (6O9C), Cyclin B1 (4Y72), HPV E6 (4GIZ), and EGFR (1M17)

showed docking scores of -4.2, -6.7, -5.5, -6.1, -4.3, -4.8 kcal/mol respectively. The strongest predicted interaction was observed with HER2, followed by Cyclin B1 and β-catenin, whereas BRCA1 showed the lowest docking score. Eicosene occupied the predicted binding pockets and interacted with several residues of the respective target proteins. Detailed docking parameters and interacting residues are presented in Table 8, while the corresponding two-dimensional and three-dimensional interaction poses are shown in Figure 5. Overall, the docking results indicate favourable interactions of eicosene with multiple cancer-associated targets and provide computational support for its further investigation in anticancer studies.

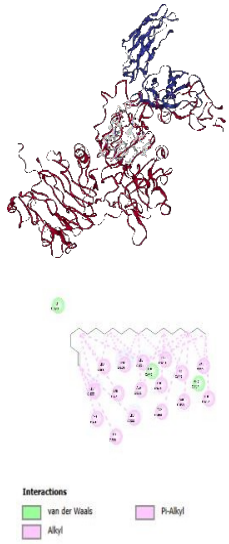
Table 8. Docking results of 5- Eicosene complex with selected anticancer protein targets.

S. No	**Ligand-Protein (PDB Id)**	**Vina Score**	**Cavity Volume**	**Centres XYZ**	**Docking Box XYZ**	**Residues**
1.	5-Eicosene - **1Y98**	-4.2	923	-27,51,0	27,27,27	**Chain A:** VAL1654 SER1655 GLY1656 LEU1657 THR1658 PRO1659 PHE1662 MET1663

						ASN1678 LEU1679 THR1700 LEU1701 LYS1702 **Chain B:** SER5 PRO7
2.	5-Eicosene - **5KWG**	-6.7	1037	43,24,-36	27,27,27	**Chain C:** LEU388 ILE390 LEU400 PHE403 LEU406 LEU421 THR422 LEU423 LEU431 LEU433 ALA444 LEU445 ILE446 LEU452 CYS453 PHE454 VAL455 VAL458 TRP460 LEU471 TRP499
3.	5-Eicosene - **6O9C**	-5.5	759	66,16,15	27,27,27	**Chain A:** ARG6 PHE8 TYR27 ASP29 ASP30 GLN32 THR233 PRO235 PHE241 **Chain B:** TYR46 SER72 ASP73 PHE76 SER77 TYR83 LEU85
4.	5-Eicosene - **4Y72**	-6.1	1535	29,-66,190	27,27,27	**Chain A:** ILE10 TYR15 VAL18 ALA31 LYS33 GLU51 VAL64
						PHE80 GLU81 PHE82 LEU83 SER84 MET85 ASP86 GLN132 ASN133 LEU134 LEU135 ALA145 ASP146
5.	5-Eicosene - **4GIZ**	-4.3	366	-22, 67, -25	27, 27, 27	**Chain B:** VAL30 TYR31 PHE44 LEU49 CYS50 VAL52 ALA60 VAL61 CYS65 LEU66 TYR69 SER70 SER73 GLN106 ARG128 ARG130
6.	5-Eicosene - **1M17**	-4.8	991	36, 8, 51	27, 27, 27	**Chain A:** PHE699 VAL702 ALA719 ILE720 LYS721 LEU723 GLU738 THR766 LEU820 THR830 ASP831



5-eicosene -**1Y98**



5-eicosene -**5KWG**

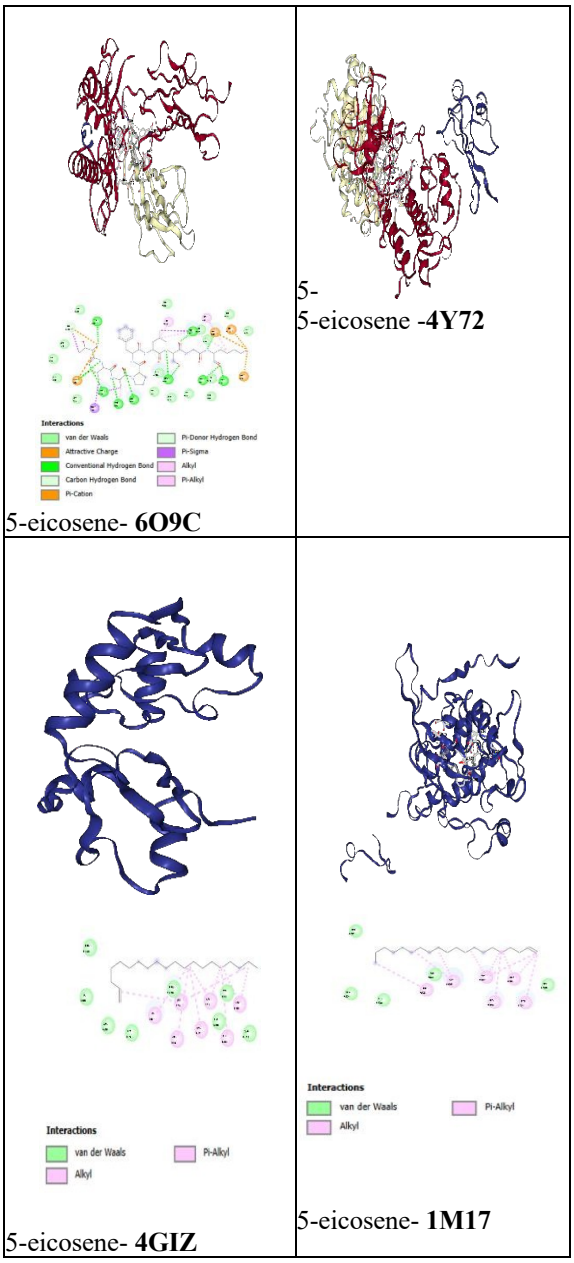


Figure 5. 3D and 2D interaction plots illustrating the binding interactions of 5-eicosene within the active sites of the anticancer target proteins.

Computational methods are widely utilised in the contemporary process of discovering drugs, expediting the search for therapeutic agents and the screening process before empirical verification. Among the numerous computational methodologies, molecular docking has been predominantly adopted for the prediction of the binding modes, interaction patterns and the binding energies of small molecules with target proteins for drug design and discovery [19,29]. In a docking process, each ligand is scanned in multiple conformers inside the receptor binding pocket and is scored based on the predicted binding free energy; in general, the more negativedocking scores imply more stable and thermodynamically favourable interactions between the protein and the ligand, thus more likely to exhibit biological activity [30,31].

Similar studies reported that phytochemicals with docking scores in the range of -6.0 to -10.0 kcal/mol showed positive interactions with cancer target proteins and can be treated as potential hit or lead molecules in the discovery of anticancer drugs [19]. The utility of molecular docking for identifying the phytochemicals with multiple targets in cancer pathways was highlighted by Sharma et al. [32]. The findings indicated that the chosen phytocompounds have beneficial interactions with many cancer-related target proteins (namely in breast, gastric, and cervical cancers), corroborating the previous results.

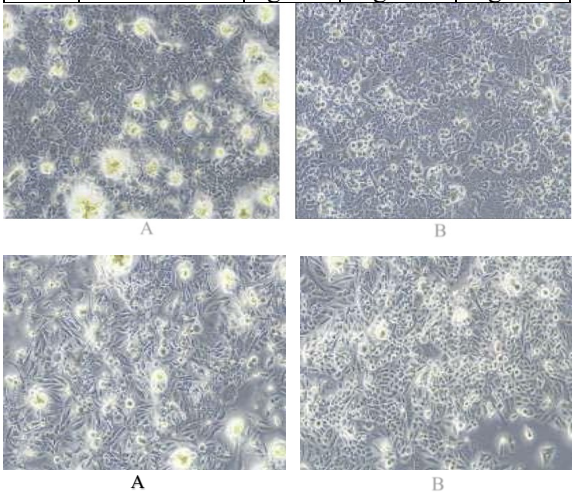
INVITRO CYTOTOXIC ACTIVITY

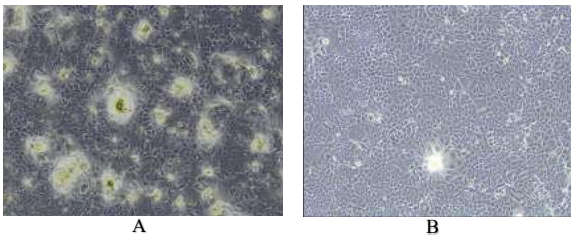
The invitro cytotoxic activity of the methanolic root extract of *C. argentea* was assessed against three human cancer cell lines, namely, MCF-7, Hep3B, and HeLa cells, using the MTT assay. As represented in Table 9, the extract produced a concentration-dependent increase in growth inhibition in all three cell lines. HeLa cells showed the highest inhibition, reaching 44.54% at

100 µg/mL, followed by MCF-7 (30.68%) and Hep3B (23.12%). The corresponding correlation coefficients (r) were 0.9993, 0.9774, and 0.9192 for MCF-7, Hep3B, and HeLa, respectively, indicating a positive concentration–response relationship. Since growth inhibition remained below 50% at the highest tested concentration, the IC_{50} values for all three cell lines were >100 µg/Ml suggesting that the crude methanolic root extract shows moderate activity as a cytotoxic agent. Detailed concentration-wise inhibition data are presented in Table 9. Representative microscopic images of treated MCF-7, Hep3B, and HeLa cells at 6.25 and 100 µg/mL are shown in Figures 6,7,8 respectively.

Table 9. In vitro cytotoxic activity of *C. argentea* methanolic root extract on different cancer cell lines.

S. No	Extract Conc. (µg/mL)	% of Inhibition		
		MCF-7	Hep3B	Hela
1.	**6.25**	**0.00**	**0.00**	**24.90**
2.	**12.5**	2.56	3.76	32.22
3.	**25**	4.85	8.60	34.15
4.	**50**	15.38	12.99	39.02
5.	**100**	30.68	23.12	44.54
6.	**IC 50 value**	>100 µ g/ml	>100 µ g/ml	>100 µ g/ml





A B

Figure 6. Microscopic images on MCF-7 cell lines under treatment of A) 100 µ g/ml *C. argentea* root methanolic extract B) 6.25 µ g/ml *C. argentea* root methanolic extract.

A

B

Figure 7. Microscopic images on Hep3B cell lines under treatment of A) 100 µ g/ml *C. argentea* root methanolic extract B) 6.25 µ g/ml *C. argentea* root methanolic extract.

B

Figure 8. Microscopic images on Hela cell lines under treatment of A) 100 µ g/ml *C. argentea* root methanolic extract B) 6.25 µ g/ml *C. argentea* root methanolic extract.

This report is in concordance with earlier reports stating possible anticancer activity of medicinal plant extracts against different human cancer cells. Agu et al. [33] reconfirmed the anticancer potentials of plant phytochemicals in the attenuation of cell proliferation and targeting of diverse cellular signalling pathways responsible for tumour development. Similar results were obtained by Kis et al. [34], who reported significant cytotoxic effects of Populus nigra bud extract against MCF-7 breast cancer cell lines, which indicated that the MCF-7 cell line is sensitive to phytochemicals present in plants. Likewise, Sharma and Chauhan [32] also reported that phytochemically rich plant extracts have concentration-dependent cytotoxic effects on human cancer cell lines. The cytotoxic effects increase as the concentration of the extract increases. Patra et al., [35] also supported that naturally derived phytochemicals have been reported to control cancer cell proliferation by the induction of apoptosis, cell cycle arrest, and increasing reactive oxygen species (ROS) and regulating different signalling pathways linked with cancer initiation and development. Moreover, Kalsoom et al. [36] also showed cytotoxic activity of *Caladium lindenii* against HeLa cancer cells; there was concentration-dependent cell killing, and cellular changes suggested apoptosis. Newman and Cragg [2] confirmed the continued significance of natural products as one of the most prolific sources of a large number of structurally diverse chemical compounds with substantial anticancer activity.

CONCLUSION

The present study comprehensively evaluated the phytochemical constituents and anticancer potential of the methanolic root extract of *Celosia argentea* through GC-MS, molecular docking, and in vitro cytotoxic study. GC–MS profiling of the methanolic root extract shows different classes of phytochemicals such as steroids, terpenoids, fatty acid derivatives, hydrocarbons, esters, and other secondary metabolites. Amongst the phytoconstituents present, Ergostane-3,5,6,12,25-pentol,25-acetate, 1-methyldecahydronaphthalene, methyl stearate and 5-eicosene were subjected to molecular docking against anticancer key target proteins like BRCA1, HER2, β-catenin, Cyclin B1, HPV E6 and EGFR, where they show good protein-ligand interactions, which indicate their ability to target the various molecular signalling pathways for cancer. The methanolic root extract also showed good cytotoxic effect on MCF-7, Hep3B, and HeLa cell lines in a dose-dependent manner and more potency towards HeLa cell lines. The correlation between the concentration of the extract and inhibition percentage is positive and indicates that the extract can inhibit cancer cell growth dose dependently. Overall, it has been concluded that *C. argentea* root is a valuable source of phytoconstituents with multi-target anticancer properties, and the study also suggests bioassay-guided isolation of active constituents, mechanism of action, pharmacological validation and preclinical evaluation for clinical use as an anticancer drug.

REFERENCES

1. Hanahan, D. (2022). Hallmarks of cancer: New dimensions. *Cancer Discovery, 12*(1), 31–46.
2. Newman, D. J., & Cragg, G. M. (2020). Natural products as sources of new drugs over nearly four decades (1981–2019). *Journal of Natural Products, 83*(3), 770–803.
3. Atanasov, A. G., Zotchev, S. B., Dirsch, V. M., & International Natural Product Sciences Taskforce. (2021). Natural products in drug discovery: Advances and opportunities. *Nature Reviews Drug Discovery, 20*, 200–216.
4. Fabricant, D. S., & Farnsworth, N. R. (2001). The value of plants used in traditional medicine for drug discovery. *Environmental Health Perspectives, 109*(Suppl. 1), 69–75.
5. Cragg, G. M., & Newman, D. J. (2013). Natural products: A continuing source of novel drug leads. *Biochimica et Biophysica Acta (BBA)—General Subjects, 1830*(6), 3670–3695.
6. Harvey, A. L., Edrada-Ebel, R., & Quinn, R. J. (2015). The re-emergence of natural products for drug discovery in the genomics era. *Nature Reviews Drug Discovery, 14*, 111–129.
7. Greenwell, M., & Rahman, P. K. S. M. (2015). Medicinal plants: Their use in anticancer treatment. *International Journal of Pharmaceutical Sciences and Research, 6*(10), 4103–4112.
8. Khan, M. A., et al. (2022). Anticancer potential of *Phoenix dactylifera* L. seed extract in human cancer cells and pro-apoptotic effects mediated through caspase-3 dependent pathway in human breast cancer MDA-MB-231 cells: An in vitro and in silico investigation. *BMC Complementary Medicine and Therapies, 22*, Article 68.
9. Yang, Z.-J., Huang, S.-Y., Zhou, D.-D., Xiong, R.-G., Zhao, C.-N., Fang, A.-P., Zhang, Y.-J.,

Li, H.-B., & Zhu, H.-L. (2022). Effects and mechanisms of curcumin for theprevention and management of cancers: An updated review. *Antioxidants, 11*(8), Article 1481.

10. Kinghorn, A. D., Pan, L., Fletcher, J. N., & Chai, H. (2011). The relevance of higher plants in lead compound discovery programs. *Journal of Natural Products, 74*(6), 1539–1555.

11. Cragg, G. M., & Pezzuto, J. M. (2016). Natural products as a vital source for the discovery of cancer chemotherapeutic and chemopreventive agents. *Medical Principles and Practice, 25*(Suppl. 2), 41–59.

12. Lim, T. K. (2014). *Edible medicinal and non-medicinal plants: Volume 7, flowers*. Springer.

13. Tang, Y., Xin, H.-L., & Guo, M.-L. (2016). Review on research of the phytochemistry and pharmacological activities of *Celosia argentea*. *Revista Brasileira de Farmacognosia, 26*(6), 787–796.

14. Li, S. (2023). Research progress on chemical constituents and pharmacological effects of *Celosia* L. *Chinese Medicine, 14*, 255–266.

15. Sasidharan, S., Chen, Y., Saravanan, D., Sundram, K. M., & Yoga Latha, L. (2011). Extraction, isolation and characterization of bioactive compounds from plants' extracts. *African Journal of Traditional, Complementary and Alternative Medicines, 8*(1), 1–10.

16. Berman, H. M., Westbrook, J., Feng, Z., Gilliland, G., Bhat, T. N., Weissig, H., Shindyalov, I. N., & Bourne, P. E. (2000). The Protein Data Bank. *Nucleic Acids Research, 28*(1), 235–242.

17. Kim, S., Chen, J., Cheng, T., Gindulyte, A., He, J., He, S., Li, Q., Shoemaker, B. A., Thiessen, P. A., Yu, B., Zaslavsky, L., Zhang, J., & Bolton, E. E. (2023). PubChem 2023 update. *Nucleic Acids Research, 51*(D1), D1373–D1380.

18. Morris, G. M., Huey, R., Lindstrom, W., Sanner, M. F., Belew, R. K., Goodsell, D. S., & Olson, A. J. (2009). AutoDock4 and AutoDockTools4: Automated docking with selective receptor flexibility. *Journal of Computational Chemistry, 30*(16), 2785–2791.

19. Trott, O., & Olson, A. J. (2010). AutoDock Vina: Improving the speed and accuracy of docking with a new scoring function, efficient optimization, and multithreading. *Journal of Computational Chemistry, 31*(2), 455–461.

20. Meng, X.-Y., Zhang, H.-X., Mezei, M., & Cui, M. (2011). Molecular docking: A powerful approach for structure-based drug discovery. *Current Computer-Aided Drug Design, 7*(2), 146–157.

21. Schrödinger, LLC. (2023). *The PyMOL molecular graphics system* (Version 3.0) [Computer software].

22. Mosmann, T. (1983). Rapid colorimetric assay for cellular growth and survival: Application to proliferation and cytotoxicity assays. *Journal of Immunological Methods, 65*(1–2), 55–63.

23. Freshney, R. I. (2021). *Culture of animal cells: A manual of basic technique and specialized applications* (8th ed.). Wiley-Blackwell.

24. van Meerloo, J., Kaspers, G. J. L., & Cloos, J. (2011). Cell sensitivity assays: The MTT assay. *Methods in Molecular Biology, 731*, 237–245.

25. Adams, R. P. (2007). *Identification of essential oil components by gas chromatography/mass spectrometry* (4th ed.). Allured Publishing Corporation.

26. Azwanida, N. N. (2015). A review on extraction methods used in medicinal plants: Principle, strength and limitation. *Medicinal & Aromatic Plants, 4*, Article 196.

27. Chemat, F., Vian, M. A., & Cravotto, G. (2012). Green extraction of natural products: Concept and principles. *International Journal of Molecular Sciences, 13*(7), 8615–8627.

28. Sharma, P., Saini, S., Hasanpuri, P., Kataria, N., & Sharma, A. (2025). Phytochemical profiling of *Celosia argentea* L. using spectroscopic techniques and evaluation of antioxidant activity. *Chemistry & Biodiversity, 22*.

29. Pinzi, L., & Rastelli, G. (2019). Molecular docking: Shifting paradigms in drug discovery. *International Journal of Molecular Sciences, 20*(18), Article 4331.

30. Ferreira, L. G., dos Santos, R. N., Oliva, G., & Andricopulo, A. D. (2015). Molecular docking and structure-based drug design strategies. *Molecules, 20*(7), 13384–13421.

31. Pagadala, N. S., Syed, K., & Tuszynski, J. (2017). Software for molecular docking: A review. *Biophysical Reviews, 9*, 91–102.

32. Sharma, A. D., & Chauhan, A. (2024). Unlocking the anti-cancer potential of phytocompounds from essential oils using molecular docking and in vitro validation. *Discover Plants, 1*, Article 44.

33. Agu, P. C., Afiukwa, C. A., Orji, O. U., et al. (2023). Molecular docking as a tool for the discovery of molecular targets of nutraceuticals in disease management. *Scientific Reports, 13*, Article 13398.

34. Kis, B., Pavel, I. Z., Avram, S., Moaca, E. A., San Juan, M. H., Schwiebs, A., Radeke,
H. H., Muntean, D., Diaconeasa, Z., Minda, D., Oprean, C., Bojin, F., Dehelean, C. A., Soica, C., & Danciu, C. (2022). Antimicrobial activity, in vitro anticancer effect (MCF-7 breast cancer cell line), antiangiogenic and immunomodulatory potentials of *Populus nigra* L. buds extract. *BMC Complementary Medicine and Therapies, 22*, Article 74.

35. Patra, S., Pradhan, B., Nayak, R., Behera, C., Das, S., Patra, S. K., Efferth, T., Jena, M., & Bhutia, S. K. (2021). Dietary polyphenols in chemoprevention and synergistic effect in cancer: Clinical evidences and molecular mechanisms of action. *Phytomedicine, 90*, Article 153554.

36. Kalsoom, A., Altaf, A., Sarwar, M., Maqbool, T., Ashraf, M. A. B., Sattar, H., Shabbir, G., Ali, Q., & Javed, M. A. (2024). GC–MS analysis,

molecular docking, and apoptotic-based cytotoxic effect of *Caladium lindenii* Madison extracts toward the HeLa cervical cancer cell line. *Scientific Reports, 14*, Article 18438.